Monitoring statistics of the ERS-2 scatterometer for ESA cycle 102

(Project Ref. 18212/04/I-OL)

Hans Hersbach
European Centre for Medium-Range Weather Forecasts,
Shinfield Park, Reading, RG2 9AX, England
Tel: (+44 118) 9499476, e-mail: dal@ecmwf.int

March 15, 2005

1 Introduction

The quality of the UWI product was monitored at ECMWF for cycle 102. Results were compared to those obtained from the previous cycle, as well for data received during the nominal period in 2000 (up to cycle 59). No corrections for duplicate observations were applied.

During cycle 102 data was received between 21:02 UTC 17 January 2005 and 20:57 UTC 21 February 2005. No data was received for the 6-hourly data batch of 06 UTC 23 January 2005. For the period from 06 UTC 28 January to 18 UTC 30 January 2005 data extraction had been suspended at ECMWF due to an uncertainty on data quality had been arisen. In general, largest volumes (typically above 10,000) were received for 6-hourly data batches centered at 00 UTC and 12 UTC.

Data is being recorded whenever within the visibility range of a ground station, leading for cycle 102 to a coverage of the North-Atlantic, part of the Mediterranean, the Gulf of Mexico, and to a small part of the Pacific north-west from the US and Canada (see Figure 2).

The asymmetry between the fore and aft incidence angles showed the development of several enhanced peaks, the largest occurring on 19 January 2005. The k_p-yaw ESA flag was set accordingly.

Compared to cycle 101, the comparison of the UWI wind product with ECMWF first-guess (FG) fields showed a lower relative standard deviation (from 1.68 m/s to 1.56 m/s). It is probably related to seasonal variations of the non-global data coverage, and a similar trend was observed one year before (Figure 1). The relative bias has become less negative (from -0.80 m/s to -0.65 m/s). For winds based on

CMOD5 the negative bias was reduced as well (from -0.19 m/s to -0.08 m/s). Both relative bias levels and standard deviation are better to those for 2000 (see Figure 1).

Ocean calibration shows that both bias levels and internode differences are small and stable.

The cycle-averaged evolution of performance relative to ECMWF first-guess (FG) winds is displayed in Figure 1. Figure 2 shows global maps of the over cycle 102 averaged UWI data coverage and wind climate, Figure 3 for performance relative to FG winds.

The ECMWF assimilation system was not changed during cycle 102.

2 ERS-2 statistics from 18 January to 21 February 2005

2.1 Sigma0 bias levels

The average sigma0 bias levels (compared to simulated sigma0's based on ECMWF model FG winds) stratified with respect to antenna beam, ascending or descending track and as function of incidence angle (i.e. across-node number) is displayed in Figure 4.

Bias levels are slightly less negative to those during cycle 101, and have now become quite small. Inter-node and inter-beam dependencies are small as well, although the level of the descending mid beam is about 0.25 dB higher than that for other beams. Average bias level is around -0.25 dB, which is 0.25 dB less negative than for nominal data in 2000 (see Figure 1 of the reports for cycle 48 to 59).

The data volume of descending and ascending tracks is similar.

2.2 Incidence angles

For ESACA, across-node binning is, like the old processor, retained on a 25km mesh. From simple geometrical arguments it follows that variations in yaw attitude will lead to asymmetries between the incidence angles of the fore and aft beam. Indeed, this has been observed. Figure 5 gives a time evolution of this asymmetry, showing rapid variations, which are typical for yaw attitude errors. Also in this figure, the occasions for which the combined k_p-yaw quality flag was set are indicated by red stars. The relation with incidence-angle asymmetries is obvious. During peak events, a larger than usual amount of data was flagged as being potentially degraded.

Since the start of 2005 (see previous report), peaks had become more pronounced, reaching values of 6 degrees. During cycle 102 a few of such peaks were observed as well, the largest occurring on 19 January and 12 February 2005. The first peak might have been connected to a solar coronal mass ejection a few days before (source: www.spaceweather.com); for the event on 12 February 2005 no enhanced solar activity had been observed. Towards the end of cycle 102 amplitudes of peaks had calmed down, resulting in a behavior as observed before.

2.3 Distance to cone history

The distance to the cone history is shown in Figure 6. Curves are based on data that passed all QC, including the test on the k_p-yaw flag, however subject to the land and sea-ice check at ECMWF (see cyclic report 88 for details).

Like for cycle 101, time series are (due to lack of statistics) very noisy, especially for the first nodes. Most spikes were found to be the result of low data volumes. The data gap between 06 UTC 28 January and 18 UTC 30 January 2005 has been artificially created at ECMWF. It was triggered by an instrument anomaly in the early morning of 28 January 2005, as a result of which almost all data points were recorded as missing. Although the small amount of data that was present looked of good quality (see top panel of Figure 12), and normal observation levels were achieved soon after, it was decided at ECMWF to suspend data extraction during the weekend. Extraction was resumed on Monday morning 31 January 2005. Unfortunately the suspended data was not stored in the ECMWF archives, and, therefore, could not be monitored.

Compared to cycle 101, the average level was almost equal (from 1.19 to 1.18), and is now about 9% higher than for nominal data (see top panel Figure 1).

2.4 UWI minus First-Guess wind history

In Figure 7, the UWI minus ECMWF first-guess wind-speed history is plotted.

The history plot shows several peaks, most of which are related to low data volumes. Similar results apply for the history of de-aliased CMOD4 winds versus FG (Figure 9).

Figure 11 displays the locations for which UWI winds were more than 8 m/s weaker (top panel) and more than 8 m/s stronger (lower panel) than FG winds. Like for cycle 101, the number of such collocations is reasonably low.

In the lower panel of Figure 12 one case from the in Figure 11 shown collocations is illuminated. It shows a situation in the North Atlantic on 13 February 2005, displaying a front in the ECMWF model, associated with a patch of strong winds. The UWI product does not show this front, and winds in the south-east corner of the swath are much weaker.

Average bias levels and standard deviations of UWI winds relative to FG winds are displayed in Table 1. From this it is seen that the bias of both the UWI and CMOD4 product have become less negative, in a rather homogeneous manner. The average bias level is less negative to that for nominal data in 2000 (UWI: -0.65 m/s now, was -0.79 m/s for cycle 59). The evolution of the bias from cycles 92 to 102 is displayed in the top panel of Figure 17. The red curve is the 15-day moving average for the at ECMWF inverted ERS-2 winds; i.e., CMOD5 since 9 March 2004. Blue vertical dashed lines indicate ECMWF model changes. This plot shows that the upgoing line since end July 2004 has stabilized since November 2004. For QuikSCAT, the positive trend in the globally averaged bias of (at ECMWF inverted and bias-corrected) QuikSCAT winds (middle panel) did continue, however, showed a swift drop in January 2005.

The standard deviation of UWI winds compared to cycle 101 has become smaller

	cycle 100		cycle 102	
	UWI	CMOD4	UWI	CMOD4
speed STDV	1.68	1.66	1.56	1.55
node 1-2	1.85	1.79	1.67	1.62
node 3-4	1.70	1.68	1.57	1.55
node 5-7	1.62	1.61	1.51	1.50
node 8-10	1.56	1.54	1.50	1.50
node 11-14	1.61	1.60	1.49	1.49
node 15-19	1.65	1.65	1.51	1.51
speed BIAS	-0.80	-0.77	-0.65	-0.63
node 1-2	-1.48	-1.42	-1.27	-1.23
node 3-4	-1.13	-1.06	-0.99	-0.92
node 5-7	-0.81	-0.77	-0.70	-0.67
node 8-10	-0.60	-0.59	-0.50	-0.50
node 11-14	-0.58	-0.57	-0.42	-0.42
node 15-19	-0.57	-0.57	-0.40	-0.41
direction STDV	27.9	18.1	27.4	18.7
direction BIAS	-2.8	-3.2	-3.1	-2.8

Table 1: Biases and standard deviation of ERS-2 versus ECMWF FG winds in m/s for speed and degrees for direction.

(1.56 m/s, was 1.68 m/s) in a rather uniform way. The seasonal trend makes an objective statement on quality evolution impossible.

For cycle 102 the (UWI - FG) direction standard deviations were ranging between 15 and 40 degrees (Figure 8). Sharp peaks are the result of low data volumes. The average performance for UWI wind direction was almost unaltered (STDV 27.4 degrees, was 27.9 degrees, bias -3.1 degrees, was -2.8 degrees).

2.5 Scatterplots

Scatterplots of FG winds versus ERS-2 winds are displayed in Figures 13 to 16. Values of standard deviations and biases are slightly different from those displayed in Table 1. Reason for this is that, for plotting purposes, the in 0.5 m/s resolution ERS-2 winds have been slightly perturbed (increases scatter with 0.02 m/s), and that zero wind-speed ERS-2 winds have been excluded (decreases scatter with about 0.05 m/s).

The scatterplot of UWI wind speed versus FG (Figure 13) is very similar to that for (at ECMWF inverted) de-aliased CMOD4 winds (Figure 15). It confirms that the ESACA inversion scheme is working properly. The reduced standard deviation compared to cycle 101 (1.58 m/s, was 1.71 m/s), originates from a less intense wind climate.

Winds derived on the basis of CMOD5 are displayed in Figure 16. The relative standard deviation is lower than for CMOD4 winds (1.53 m/s versus 1.57 m/s). Compared to ECMWF FG, CMOD5 winds are -0.08 m/s slower. A large negative

bias for extreme winds, as observed for previous cycles was less present for cycle 102, resulting in a better agreement between CMOD5 and ECMWF winds in this range.

Figure Captions

Figure 1: Evolution of the performance of the ERS-2 scatterometer averaged over 5-weekly cycles from 12 December 2001 (cycle 69) to 21 February 2005 (end cycle 102) for the UWI product (solid, star) and de-aliased winds based on CMOD4 (dashed, diamond). Results are based on data that passed the UWI QC flags. For cycle 85 two values are plotted; the first value for the global set, the second one for the regional set. Dotted lines represent values for cycle 59 (5 December 2000 to 17 January 2001), i.e. the last stable cycle of the nominal period. From top to bottom panel are shown the normalized distance to the cone (CMOD4 only) the standard deviation of the wind speed compared to FG winds, the corresponding bias (for UWI winds the extreme inter-node averages are shown as well), and the standard deviation of wind direction compared to FG.

Figure 2: Average number of observations per 12H and per 125km grid box (top panel) and wind-climate (lower panel) for UWI winds that passed the UWI flags QC and a check on the collocated ECMWF land and sea-ice mask.

Figure 3: The same as Figure 2, but now for the relative bias (top panel) and standard deviation (lower panel) with ECMWF first-guess winds.

Figure 4: Ratio of $< \sigma_0^{0.625} > / <$ CMOD4(FirstGuess)$^{0.625} >$ converted in dB for the fore beam (solid line), mid beam (dashed line) and aft beam (dotted line), as a function of incidence angle for descending and ascending tracks. The thin lines indicate the error bars on the estimated mean. First-guess winds are based on the in time closest (+3h, +6h, +9h, or +12h) T511 forecast field, and are bilinearly interpolated in space.

Figure 5: Time series of the difference in incidence angle between the fore and aft beam. Red stars indicate the occurrences for which the combined k_p-yaw flag was set.

Figure 6: Mean normalized distance to the cone computed every 6 hours for nodes 1-2, 3-4, 5-7, 8-10, 11-14 and 15-19 (solid curve close to 1 when no instrumental problems are present). The dotted curve shows the number of incoming triplets in logarithmic scale (1 corresponds to 60,000 triplets) and the dashed one indicates the fraction of complete (based on the land and sea-ice mask at ECMWF) sea-located triplets rejected by ESA flags, or by the wind inversion algorithm (0: all data kept, 1: no data kept).

Figure 7: Mean (solid line) and standard deviation (dashed line) of the wind speed difference UWI - first guess for the data retained by the quality control.

Figure 8: Same as Fig. 7, but for the wind direction difference. Statistics are computed only for wind speeds higher than 4 m/s.

Figures 9 and 10: Same as Fig. 7 and 8 respectively, but for the de-aliased

CMOD4 data.

Figure 11: Locations of data during cycle 102 for which UWI winds are more than 8 m/s weaker (top panel) respectively stronger (lower panel) than FG, and on which QC on UWI flags and the ECMWF land/sea-ice mask was applied.

Figure 12: Comparison between UWI (red) and ECMWF FG (blue) winds for the only valid data observed during the 6-hourly data batch around 00 UTC 28 January 2005 (top panel) and for an Atlantic case on 13 February 2005 (lower panel).

Figure 13: Two-dimensional histogram of first guess and UWI wind speeds, for the data kept by the UWI flags, and QC based on the ECMWF ice and land and sea-ice mask. Circles denote the mean values in the y-direction, and squares those in the x-direction.

Figure 14: Same as Fig. 13, but for wind direction. Only wind speeds higher than 4m/s are taken into account.

Figure 15: Same as Fig. 13, but for de-aliased CMOD4 winds.

Figure 16: Same as Fig. 13, but for de-aliased CMOD5 winds.

Figure 17: Bias relative to FG winds of the wind speed of ERS-2 winds (based on bias-corrected CMOD4 before 9 March 2004, and on CMOD5 afterwards) for nodes 1-19 (top panel) respectively of 50-km QuikSCAT (based on the QSCAT-1 model function) for nodes 5-34 (i.e., inner-beam zone; middle and lower panels) versus ECMWF first guess for the period of cycle 92 to 102. Curves represent centered 15-day running means for the top and middle panel, and a 30-day running mean for the lower panel. Vertical dashed blue lines mark ECMWF model changes.

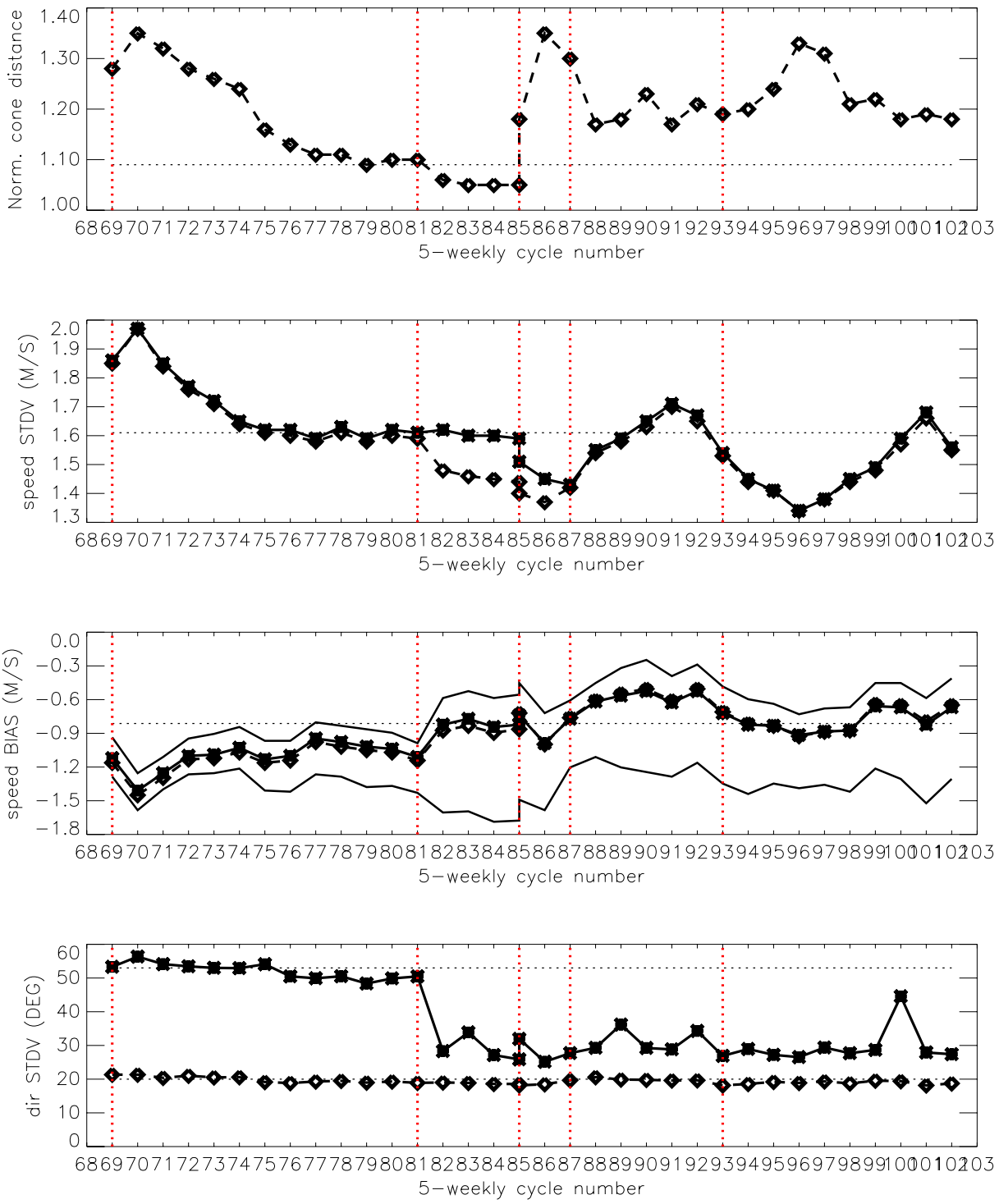
Norm. cone distance
1.40
1.30
1.20
1.10
1.00
speed STDV (M/S)
2.0
1.9
1.8
1.7
1.6
1.5
1.4
1.3
speed BIAS (M/S)
0.0
−0.3
−0.6
−0.9
−1.2
−1.5
−1.8
dir STDV (DEG)
60
50
40
30
20
10
0
5−weekly cycle number

Figure 1

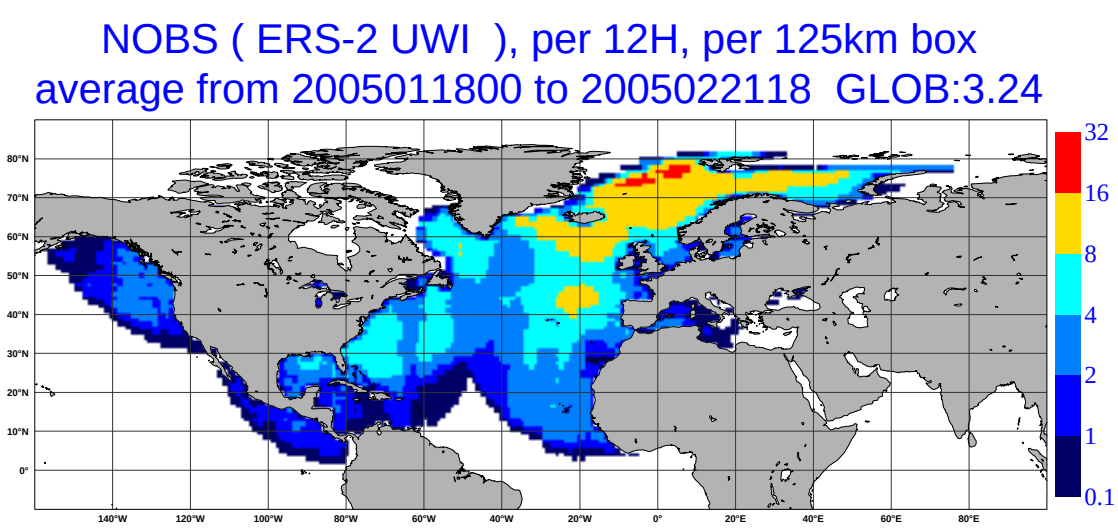
NOBS (ERS-2 UWI), per 12H, per 125km box
average from 2005011800 to 2005022118 GLOB:3.24
80°N
70°N
60°N
50°N
40°N
30°N
20°N
10°N
0°
140°W
120°W
100°W
80°W
60°W
40°W
20°W
0°
20°E
40°E
60°E
80°E
32
16
8
4
2
1
0.1

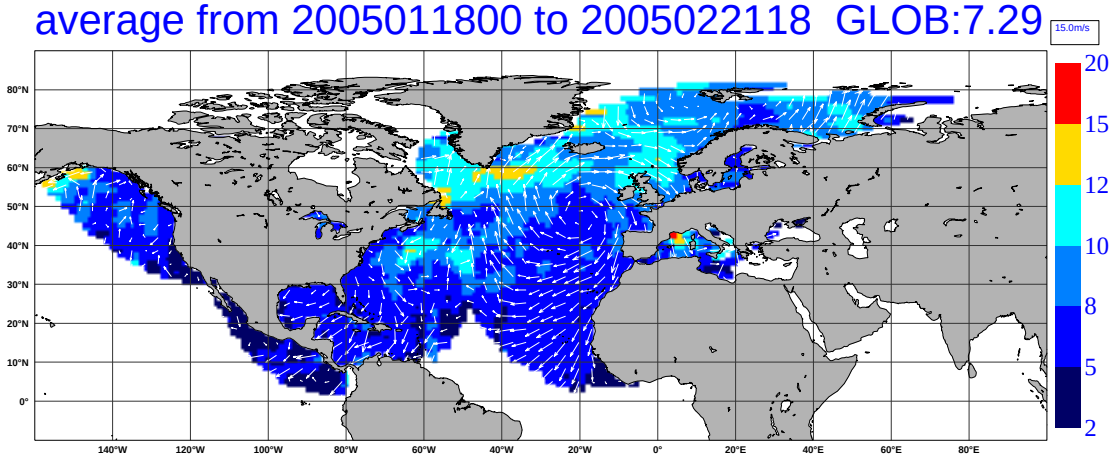
AVERAGE (ERS-2 UWI), in m/s.
average from 2005011800 to 2005022118 GLOB:7.29
15.0m/s
80°N
70°N
60°N
50°N
40°N
30°N
20°N
10°N
0°
140°W
120°W
100°W
80°W
60°W
40°W
20°W
0°
20°E
40°E
60°E
80°E
20
15
12
10
8
5
2

Figure 2

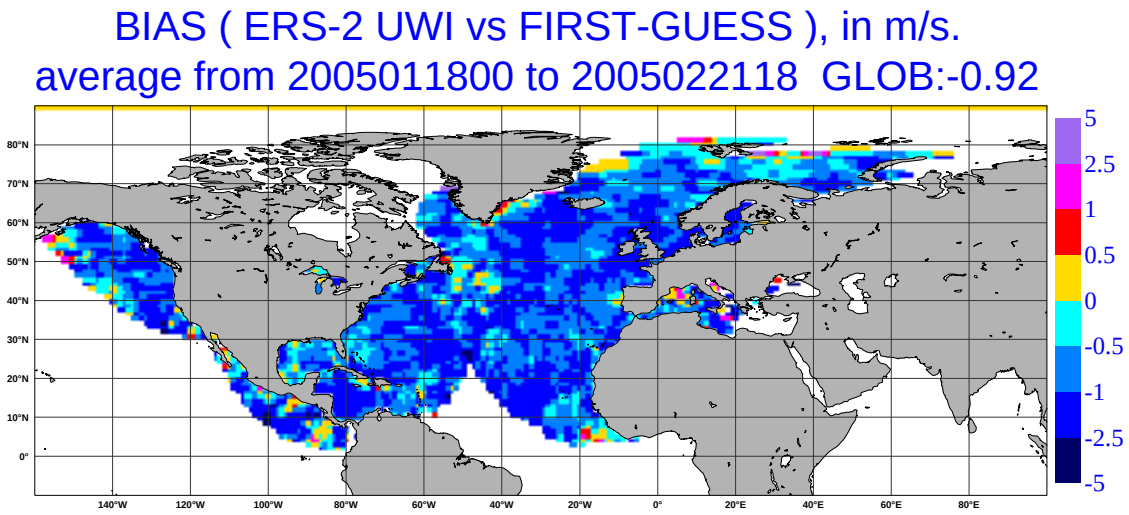
BIAS (ERS-2 UWI vs FIRST-GUESS), in m/s.
average from 2005011800 to 2005022118 GLOB:-0.92
5
2.5
1
0.5
0
-0.5
-1
-2.5
-5
80°N
70°N
60°N
50°N
40°N
30°N
20°N
10°N
0°
140°W
120°W
100°W
80°W
60°W
40°W
20°W
0°
20°E
40°E
60°E
80°E

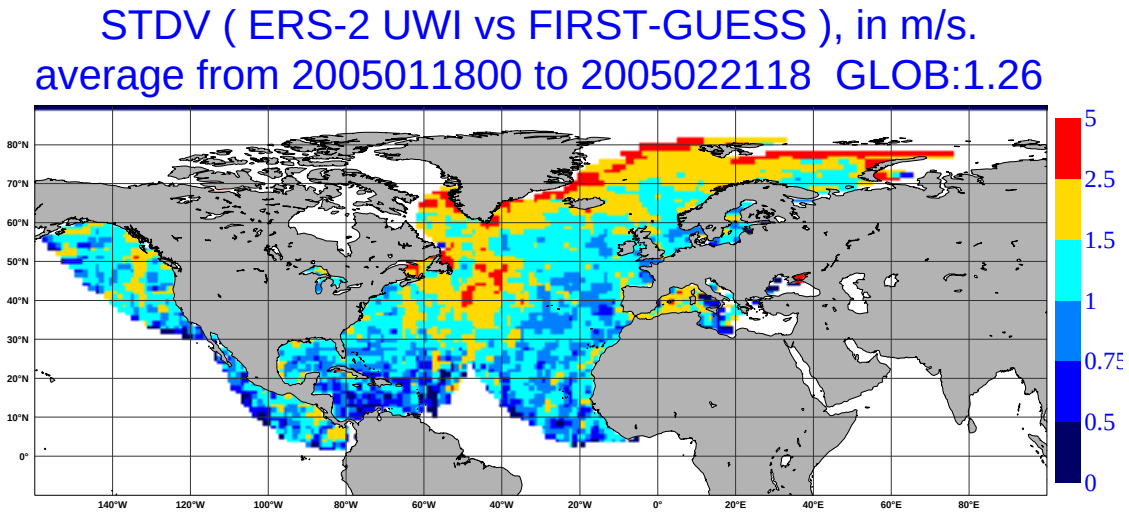
STDV (ERS-2 UWI vs FIRST-GUESS), in m/s.
average from 2005011800 to 2005022118 GLOB:1.26
5
2.5
1.5
1
0.75
0.5
0
80°N
70°N
60°N
50°N
40°N
30°N
20°N
10°N
0°
140°W
120°W
100°W
80°W
60°W
40°W
20°W
0°
20°E
40°E
60°E
80°E

Figure 3

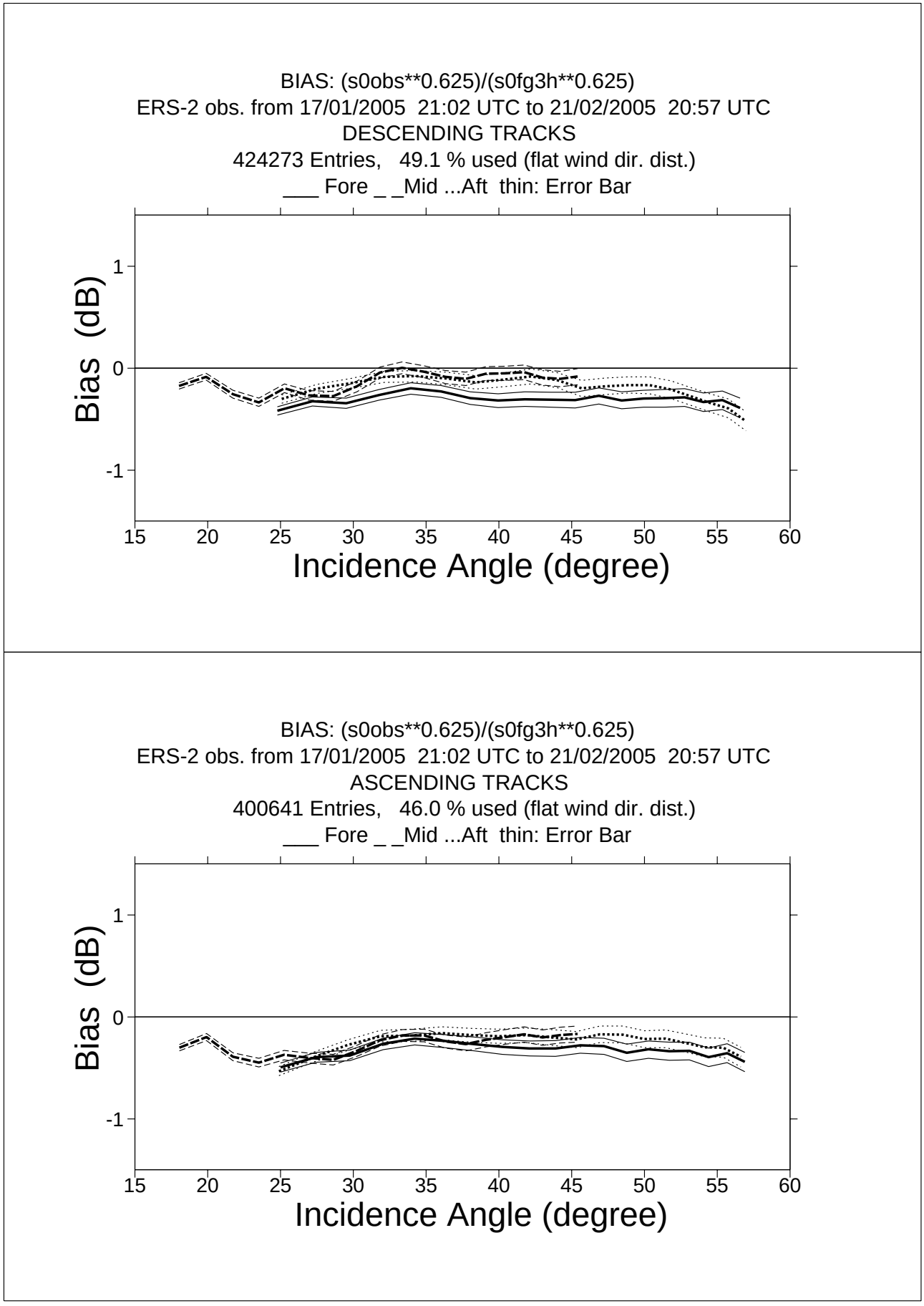
BIAS: (s0obs**0.625)/(s0fg3h**0.625)
ERS-2 obs. from 17/01/2005 21:02 UTC to 21/02/2005 20:57 UTC
DESCENDING TRACKS
424273 Entries, 49.1 % used (flat wind dir. dist.)
___ Fore _ _Mid ...Aft thin: Error Bar
Bias (dB)
1
0
-1
15
20
25
30
35
40
45
50
55
60
Incidence Angle (degree)
BIAS: (s0obs**0.625)/(s0fg3h**0.625)
ERS-2 obs. from 17/01/2005 21:02 UTC to 21/02/2005 20:57 UTC
ASCENDING TRACKS
400641 Entries, 46.0 % used (flat wind dir. dist.)
___ Fore _ _Mid ...Aft thin: Error Bar
Bias (dB)
1
0
-1
15
20
25
30
35
40
45
50
55
60
Incidence Angle (degree)

Figure 4

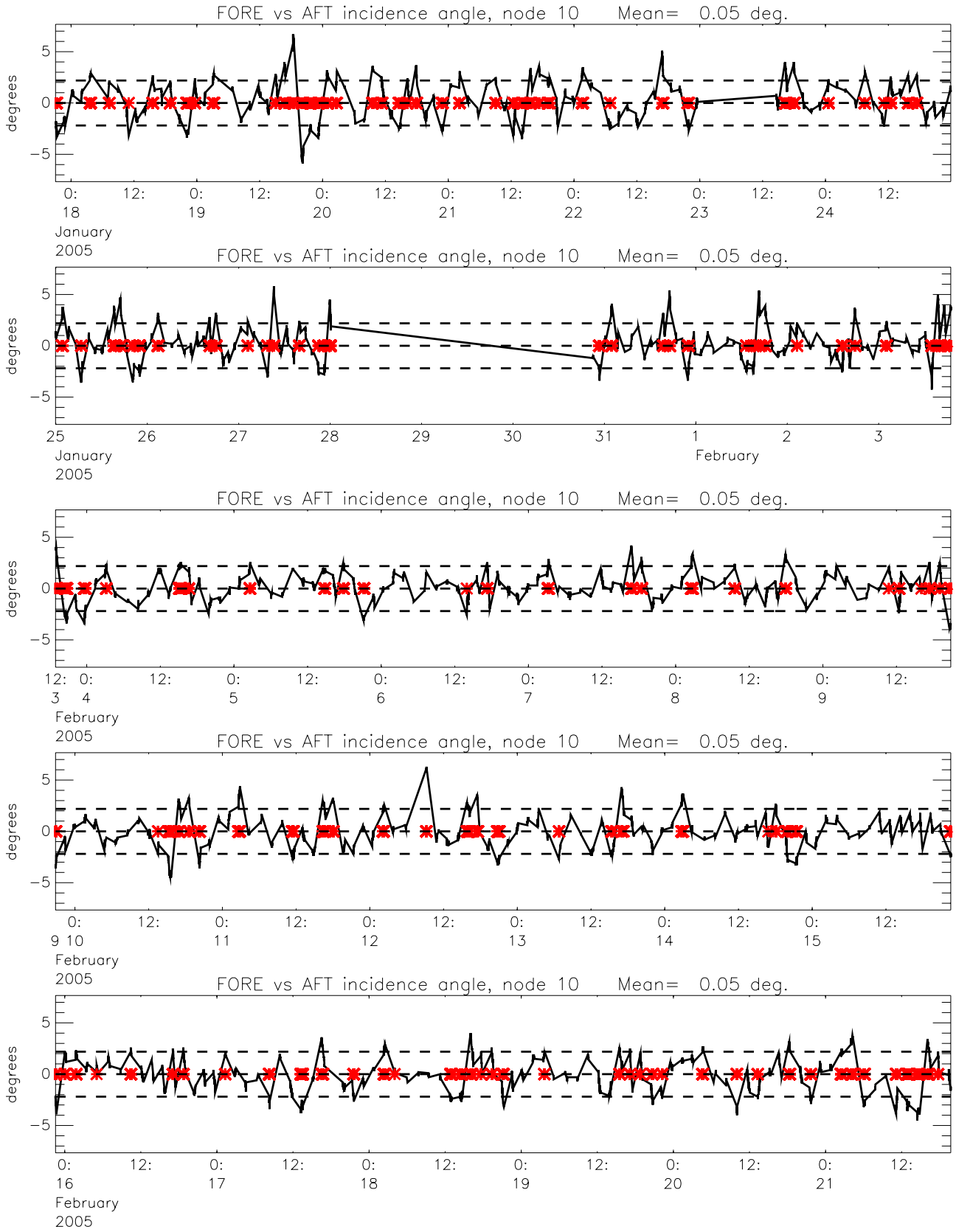
FORE vs AFT incidence angle, node 10 Mean= 0.05 deg.
degrees
5
0
−5
0: 12: 0: 12: 0: 12: 0: 12: 0: 12: 0: 12: 0: 12: 0: 12:
18 19 20 21 22 23 24
January
2005
FORE vs AFT incidence angle, node 10 Mean= 0.05 deg.
degrees
5
0
−5
25 26 27 28 29 30 31 1 2 3
January
2005
February
FORE vs AFT incidence angle, node 10 Mean= 0.05 deg.
degrees
5
0
−5
12: 0: 12: 0: 12: 0: 12: 0: 12: 0: 12: 0: 12:
3 4 5 6 7 8 9
February
2005
FORE vs AFT incidence angle, node 10 Mean= 0.05 deg.
degrees
5
0
−5
0: 12: 0: 12: 0: 12: 0: 12: 0: 12: 0: 12:
9 10 11 12 13 14 15
February
2005
FORE vs AFT incidence angle, node 10 Mean= 0.05 deg.
degrees
5
0
−5
0: 12: 0: 12: 0: 12: 0: 12: 0: 12: 0: 12:
16 17 18 19 20 21
February
2005

Figure 5

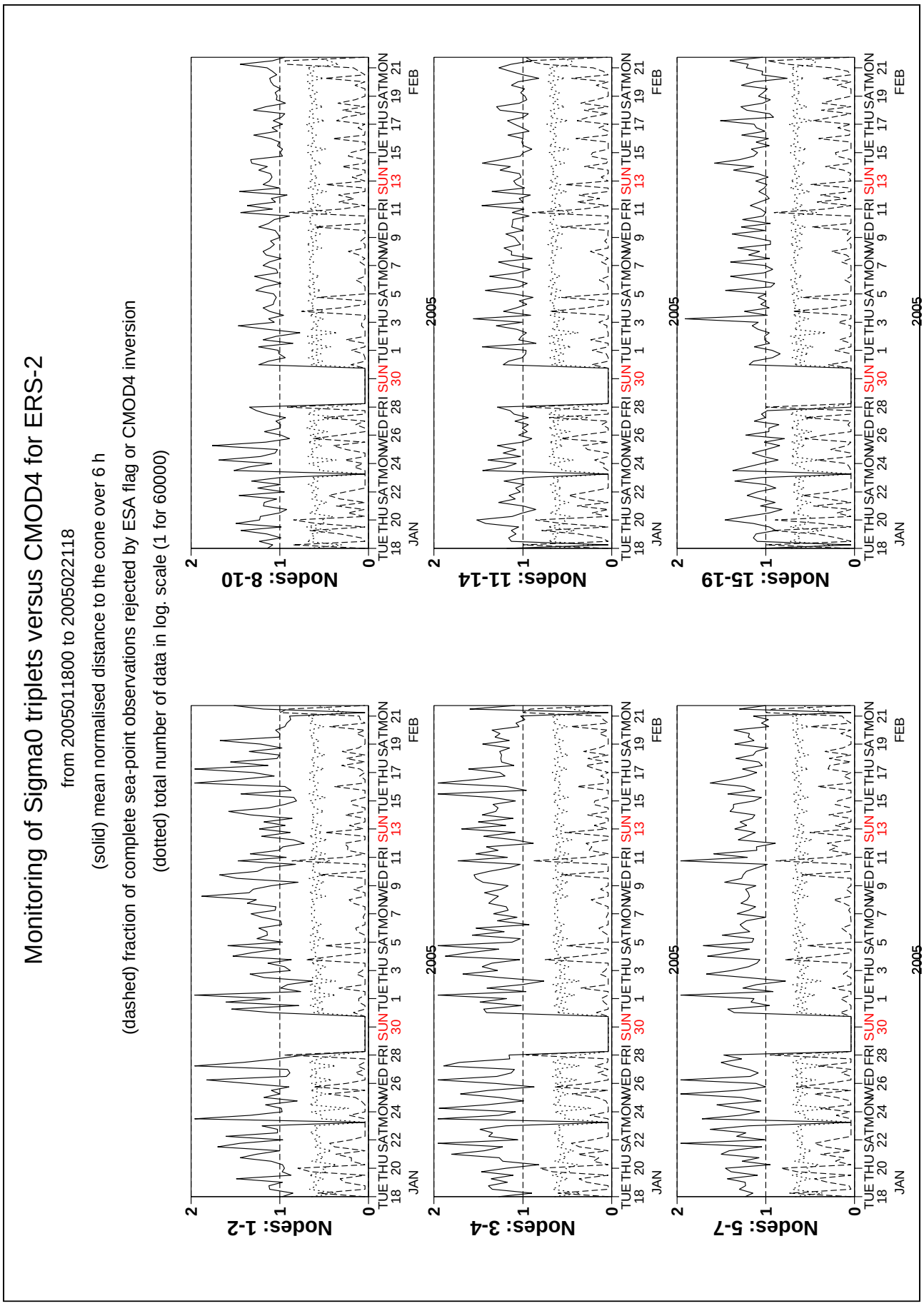
Monitoring of Sigma0 triplets versus CMOD4 for ERS-2
from 2005011800 to 2005022118
(solid) mean normalised distance to the cone over 6 h
(dashed) fraction of complete sea-point observations rejected by ESA flag or CMOD4 inversion
(dotted) total number of data in log. scale (1 for 60000)
Nodes: 1-2
Nodes: 3-4
Nodes: 5-7
Nodes: 8-10
Nodes: 11-14
Nodes: 15-19
2005
JAN
FEB

Figure 6

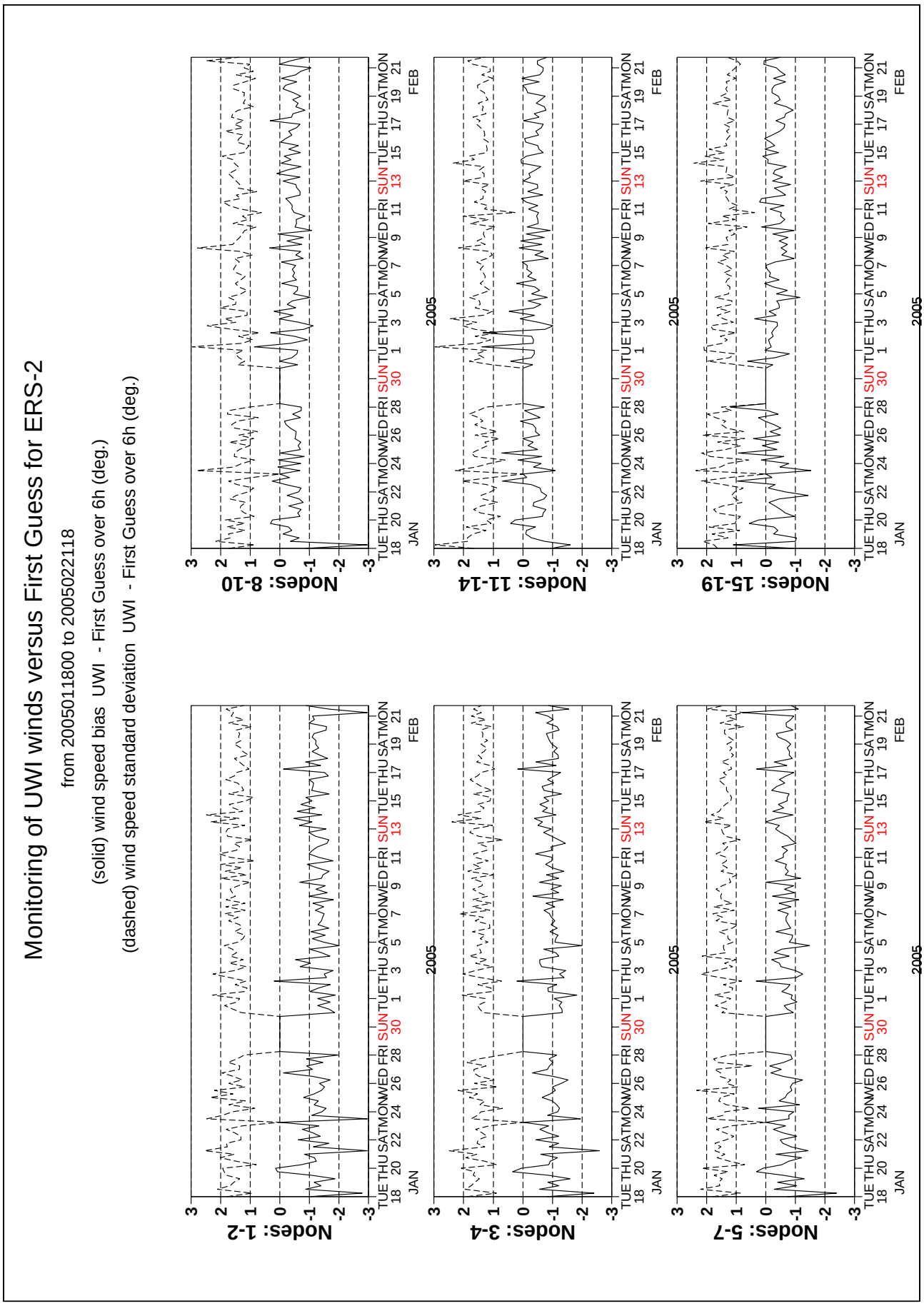
Monitoring of UWI winds versus First Guess for ERS-2
from 2005011800 to 2005022118
(solid) wind speed bias UWI - First Guess over 6h (deg.)
(dashed) wind speed standard deviation UWI - First Guess over 6h (deg.)
Nodes: 1-2
Nodes: 3-4
Nodes: 5-7
Nodes: 8-10
Nodes: 11-14
Nodes: 15-19
JAN
FEB
2005

Figure 7

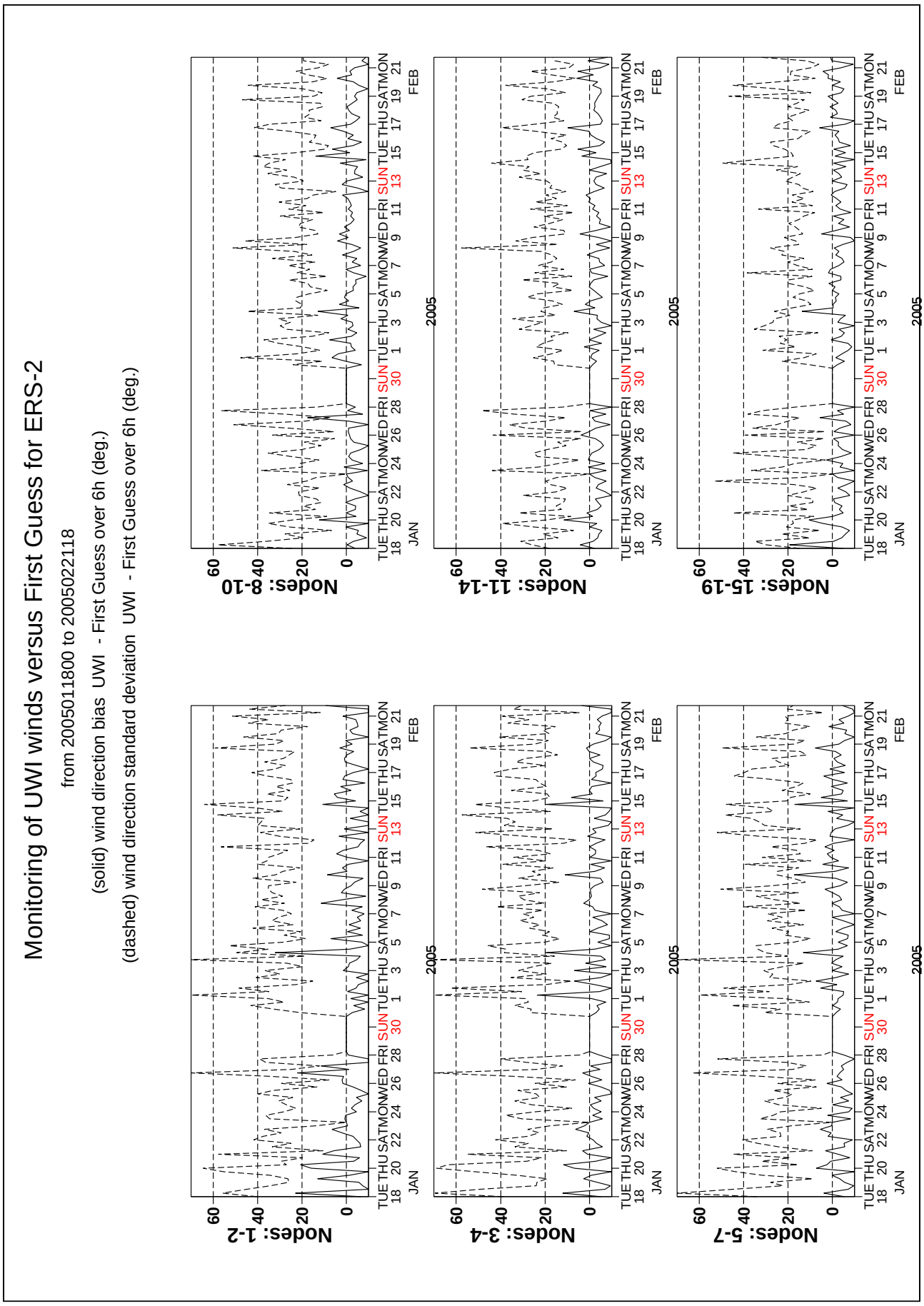
Monitoring of UWI winds versus First Guess for ERS-2
from 2005011800 to 2005022118
(solid) wind direction bias UWI - First Guess over 6h (deg.)
(dashed) wind direction standard deviation UWI - First Guess over 6h (deg.)
Nodes: 1-2
Nodes: 3-4
Nodes: 5-7
Nodes: 8-10
Nodes: 11-14
Nodes: 15-19
0
20
40
60
TUE THU SAT MON WED FRI SUN TUE THU SAT MON WED FRI SUN TUE THU SAT MON
18 20 22 24 26 28 30 1 3 5 7 9 11 13 15 17 19 21
JAN
FEB
2005

Figure 8

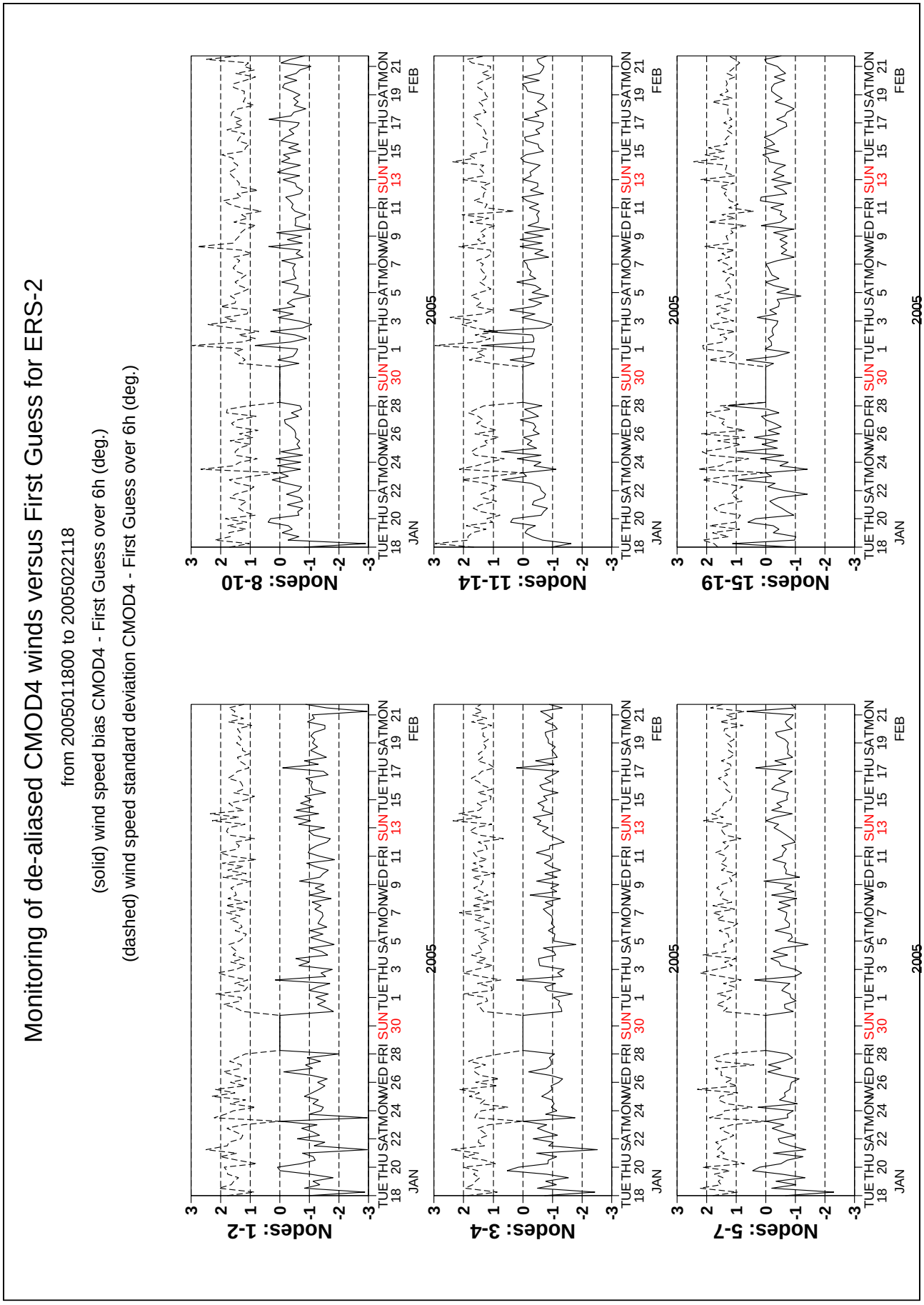
Monitoring of de-aliased CMOD4 winds versus First Guess for ERS-2
from 2005011800 to 2005022118
(solid) wind speed bias CMOD4 - First Guess over 6h (deg.)
(dashed) wind speed standard deviation CMOD4 - First Guess over 6h (deg.)
Nodes: 1-2
Nodes: 3-4
Nodes: 5-7
Nodes: 8-10
Nodes: 11-14
Nodes: 15-19
2005
JAN
FEB

Figure 9

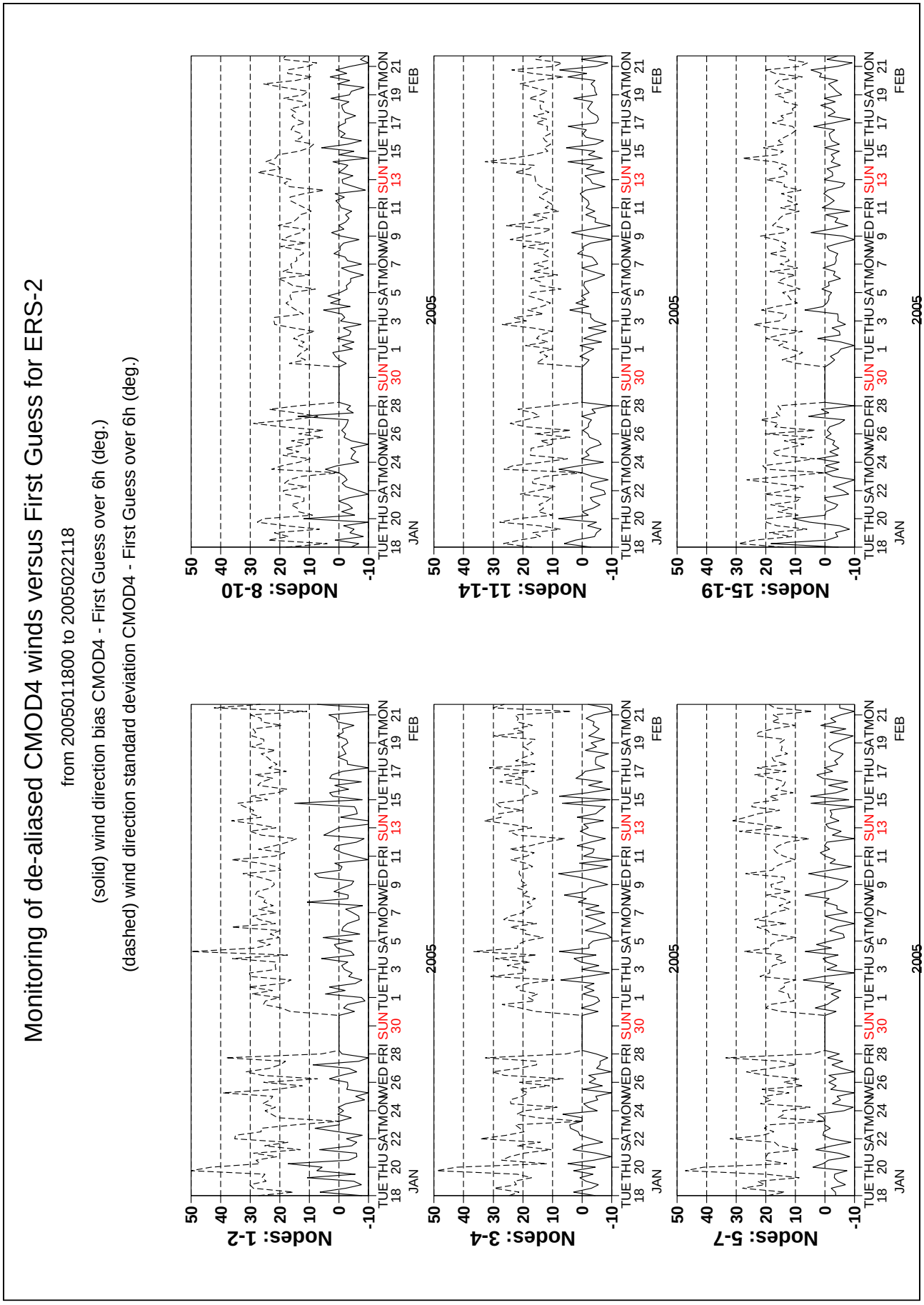
Monitoring of de-aliased CMOD4 winds versus First Guess for ERS-2
from 2005011800 to 2005022118
(solid) wind direction bias CMOD4 - First Guess over 6h (deg.)
(dashed) wind direction standard deviation CMOD4 - First Guess over 6h (deg.)
Nodes: 1-2
Nodes: 3-4
Nodes: 5-7
Nodes: 8-10
Nodes: 11-14
Nodes: 15-19
2005
JAN
FEB

Figure 10

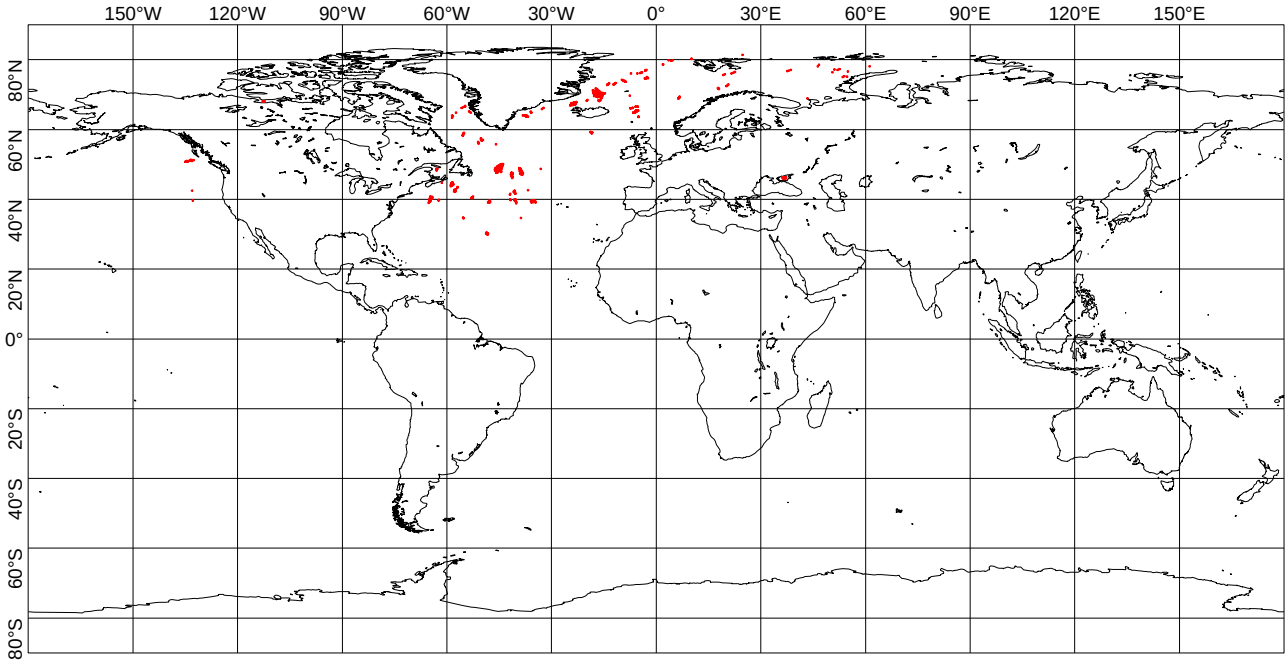
UWI winds more than 8 m/s weaker than FGAT
CYCLE 102, 2005011800 to 2005022118, QC on ESA flags
150°W
120°W
90°W
60°W
30°W
0°
30°E
60°E
90°E
120°E
150°E
80°N
60°N
40°N
20°N
0°
20°S
40°S
60°S
80°S

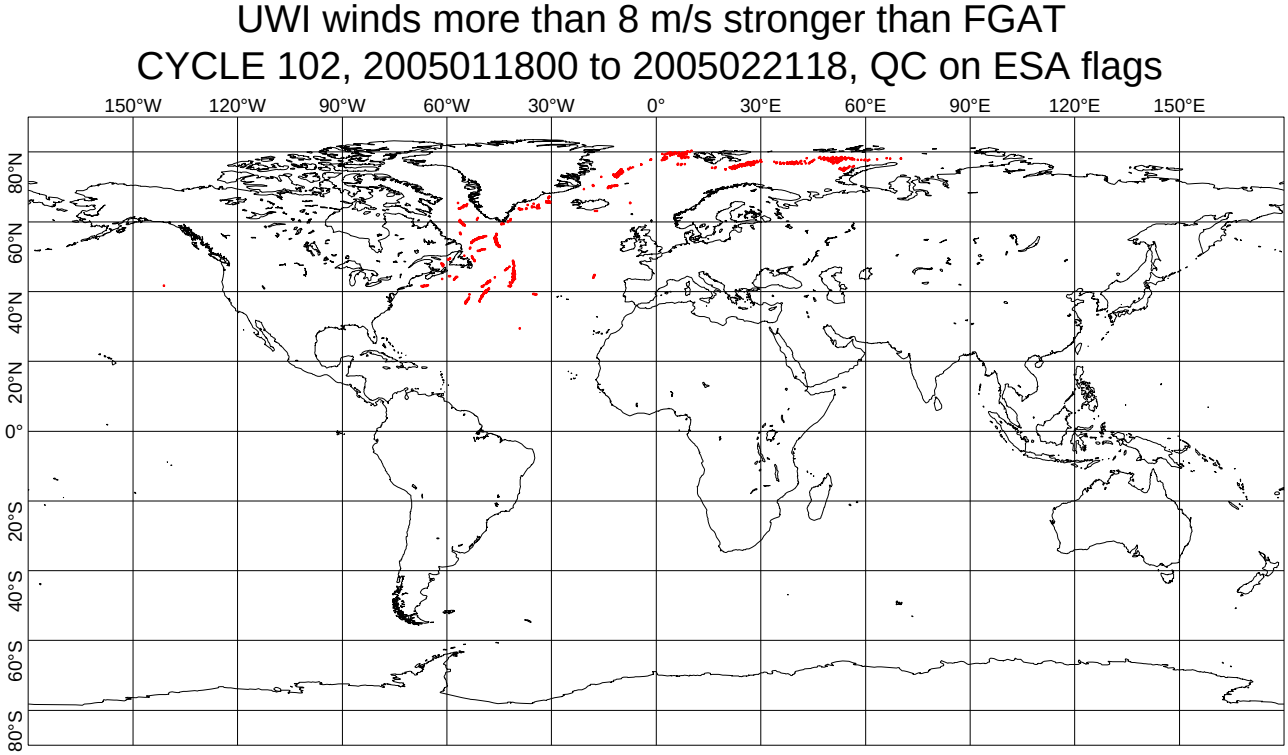
UWI winds more than 8 m/s stronger than FGAT
CYCLE 102, 2005011800 to 2005022118, QC on ESA flags
150°W
120°W
90°W
60°W
30°W
0°
30°E
60°E
90°E
120°E
150°E
80°N
60°N
40°N
20°N
0°
20°S
40°S
60°S
80°S

Figure 11

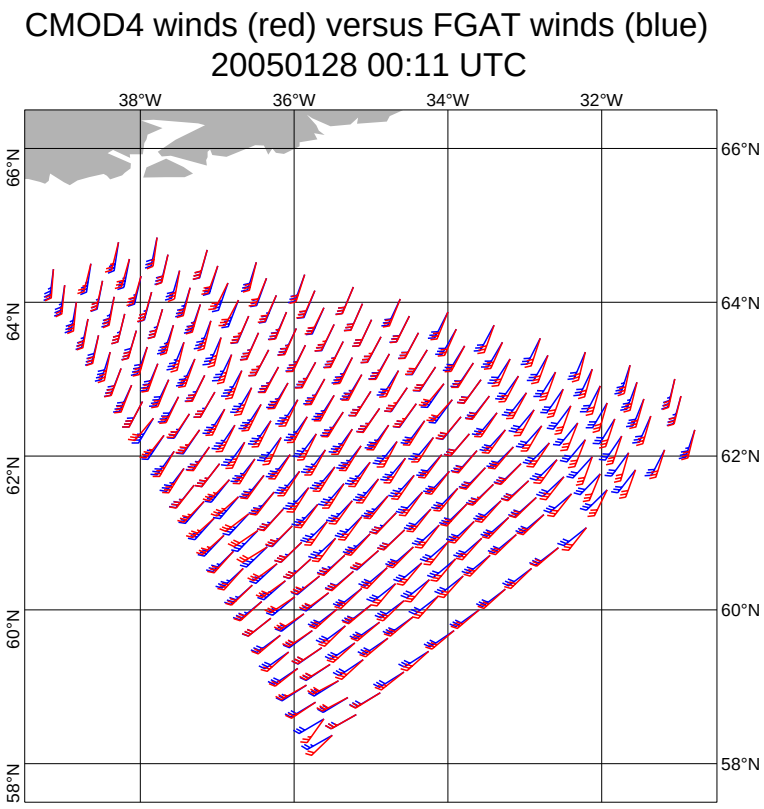
CMOD4 winds (red) versus FGAT winds (blue)
20050128 00:11 UTC
38°W
36°W
34°W
32°W
66°N
64°N
62°N
60°N
58°N

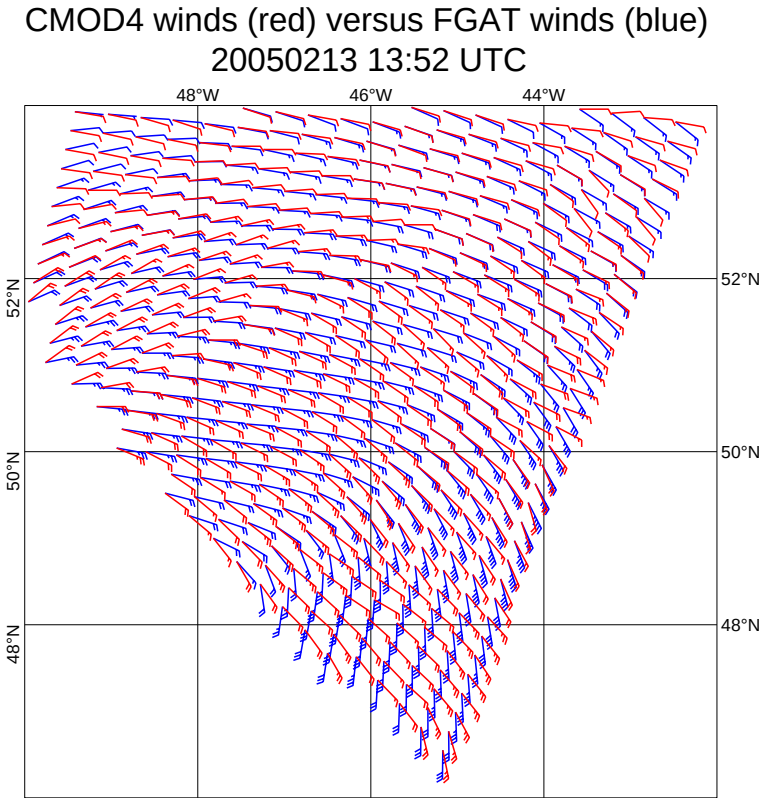
CMOD4 winds (red) versus FGAT winds (blue)
20050213 13:52 UTC
48°W
46°W
44°W
52°N
50°N
48°N

Figure 12

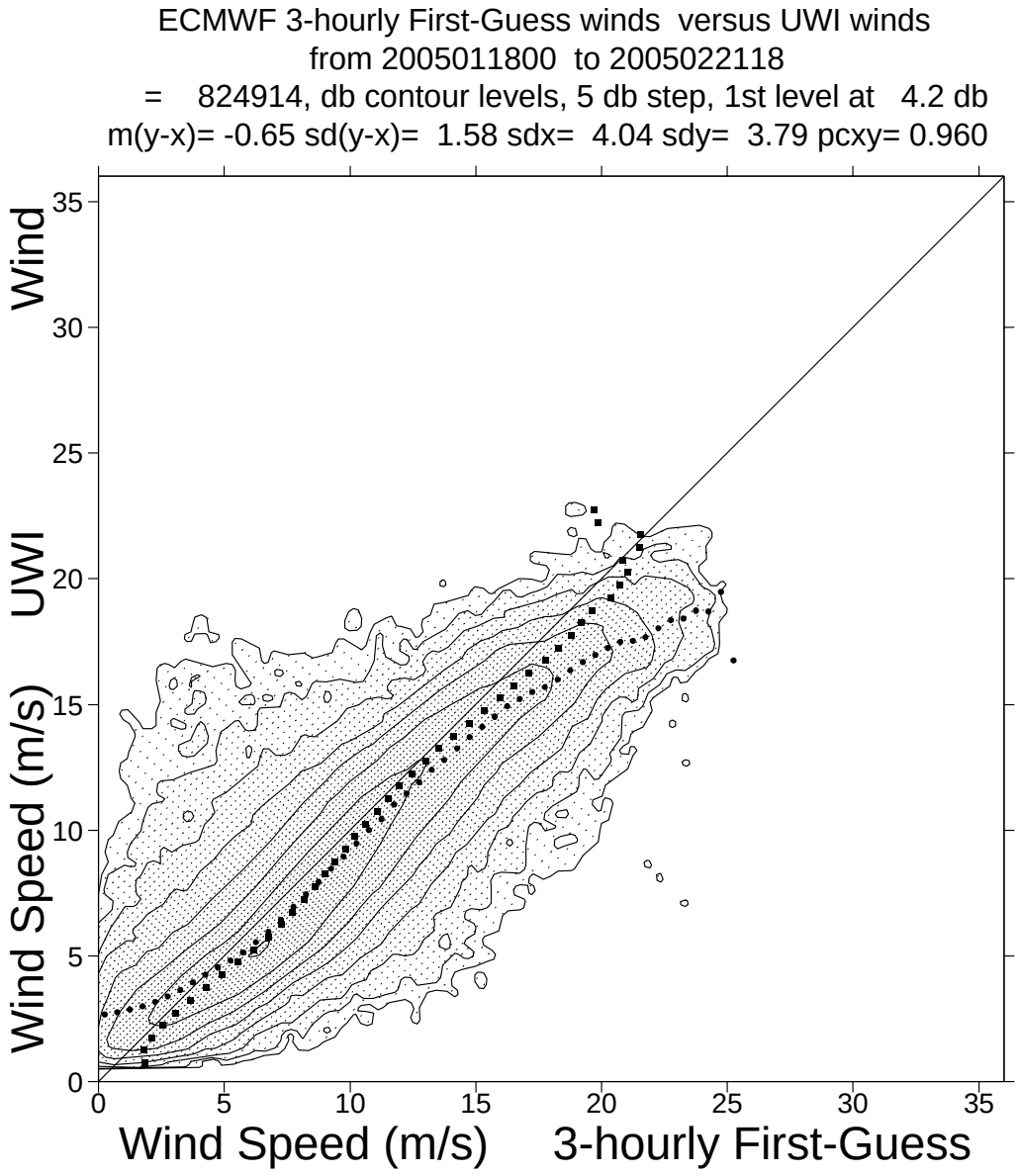
ECMWF 3-hourly First-Guess winds versus UWI winds
from 2005011800 to 2005022118
= 824914, db contour levels, 5 db step, 1st level at 4.2 db
m(y-x)= -0.65 sd(y-x)= 1.58 sdx= 4.04 sdy= 3.79 pcxy= 0.960
Wind Speed (m/s) UWI Wind
0
5
10
15
20
25
30
35
Wind Speed (m/s) 3-hourly First-Guess

Figure 13

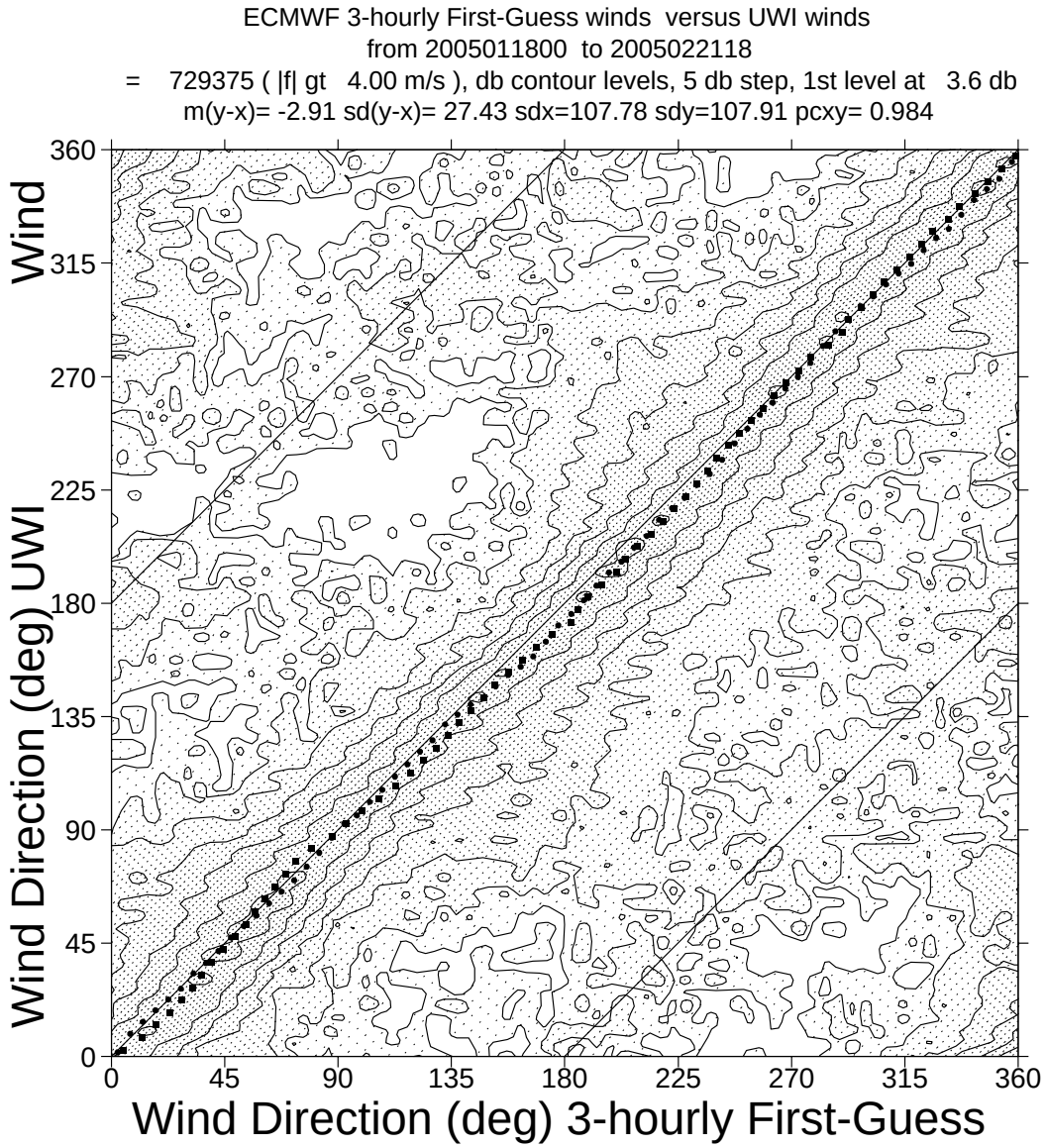
ECMWF 3-hourly First-Guess winds versus UWI winds
from 2005011800 to 2005022118
= 729375 (|f| gt 4.00 m/s), db contour levels, 5 db step, 1st level at 3.6 db
m(y-x)= -2.91 sd(y-x)= 27.43 sdx=107.78 sdy=107.91 pcxy= 0.984
Wind Direction (deg) UWI
Wind Direction (deg) 3-hourly First-Guess
0
45
90
135
180
225
270
315
360

Figure 14

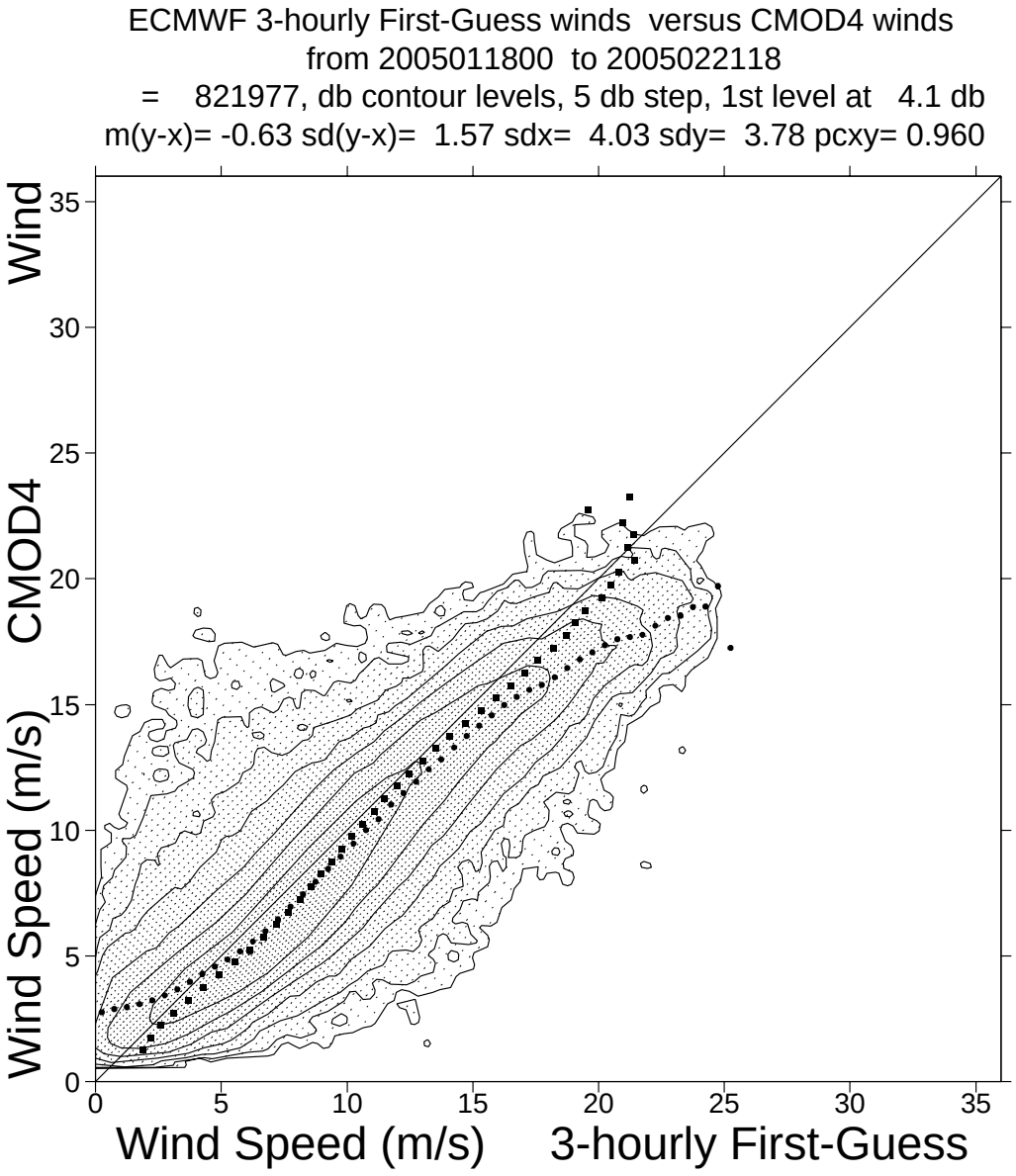
ECMWF 3-hourly First-Guess winds versus CMOD4 winds
from 2005011800 to 2005022118
= 821977, db contour levels, 5 db step, 1st level at 4.1 db
m(y-x)= -0.63 sd(y-x)= 1.57 sdx= 4.03 sdy= 3.78 pcxy= 0.960
Wind Speed (m/s) CMOD4 Wind
Wind Speed (m/s) 3-hourly First-Guess
0
5
10
15
20
25
30
35

Figure 15

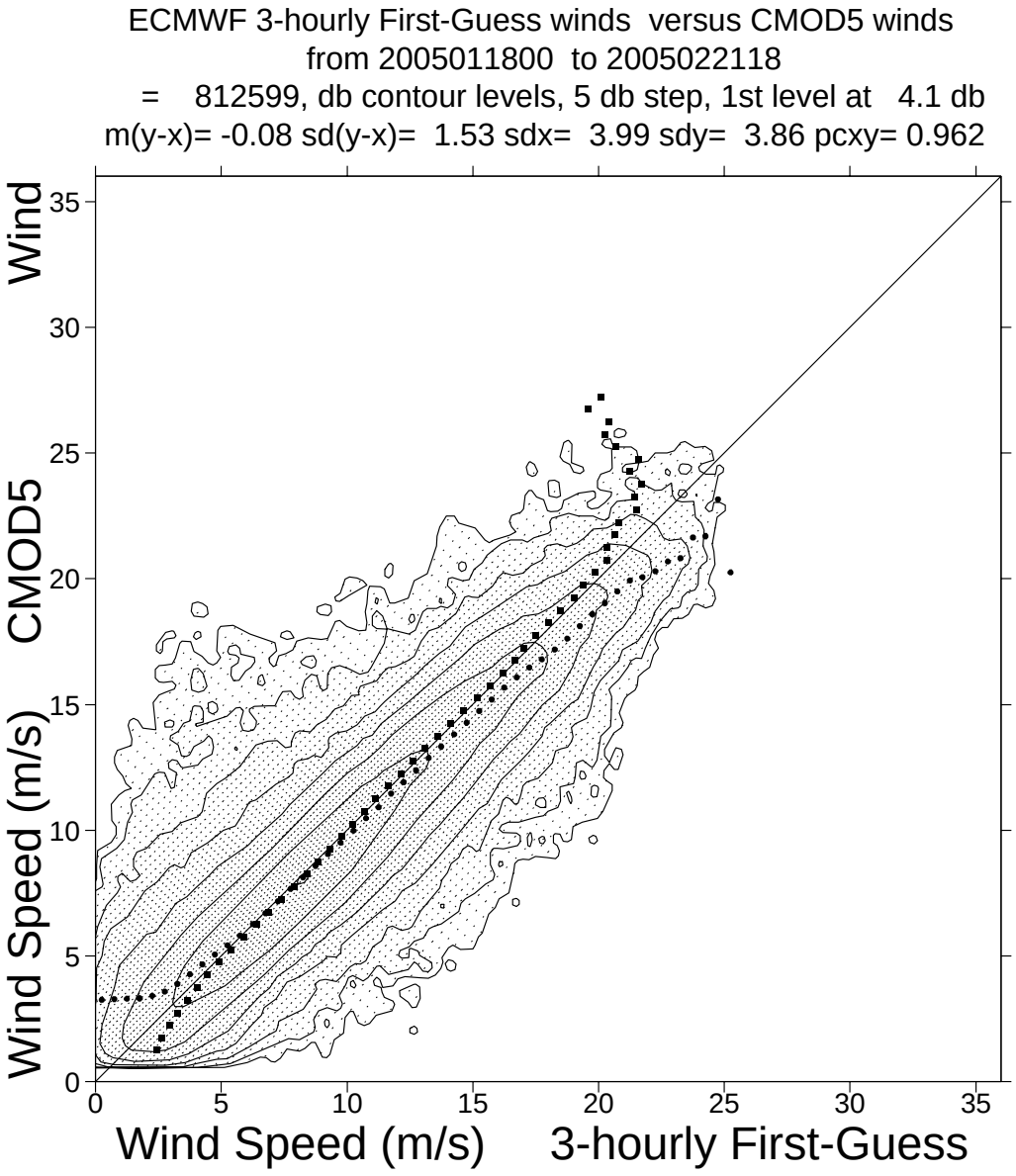
ECMWF 3-hourly First-Guess winds versus CMOD5 winds
from 2005011800 to 2005022118
= 812599, db contour levels, 5 db step, 1st level at 4.1 db
m(y-x)= -0.08 sd(y-x)= 1.53 sdx= 3.99 sdy= 3.86 pcxy= 0.962
Wind Speed (m/s) CMOD5 Wind
Wind Speed (m/s) 3-hourly First-Guess
0
5
10
15
20
25
30
35

Figure 16

ERS-2 (CMOD5)

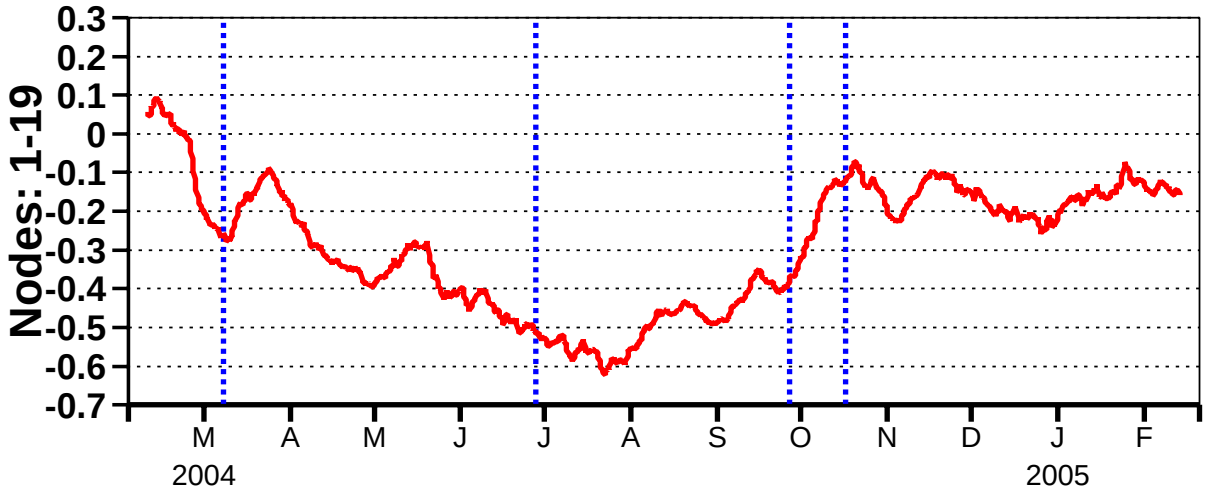

QuikSCAT (QSCAT-1)

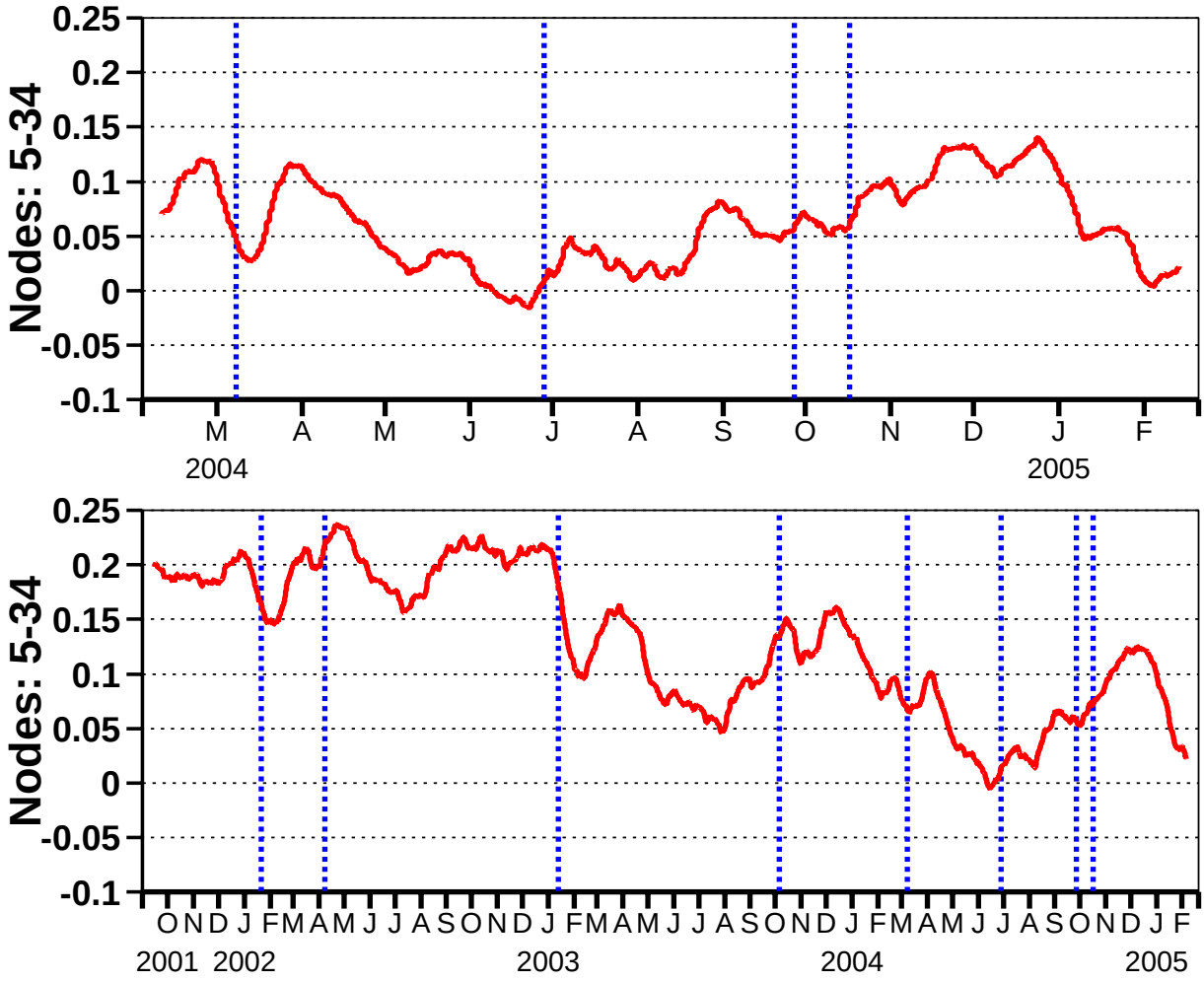

Figure 17